Final Report

December / 2023

Student Project No. CTP_FCR_2017_4

Title: Combining root architecture, root function and soil management to improve production efficiency and quality of apples

Short tittle: Improving apple rootstocks for resilience

Author: Magdalena Cobo-Medina

Supervisors: Felicidad Fernandez, Dr Richard Harrison. Dr Nicola Harrison and Dr Amanda Rasmussen

Report No: [AHDB Use only]

This is the final report of a PhD project that ran from October 2017 to November 2023. The work was funded by the Collaborative Training Partnership for Fruit Crop Research (CTP FCR) consortium: the Biotechnology and Biological Sciences Research Council (BBSRC); Berry Gardens Growers; Marks and Spencer Plc.; The National Association of Cider Makers (NACM); Worldwide Fruit Ltd.; AHDB Horticulture; The Worshipful Company of Fruiterers; and Mid-Kent Growers.

CONTENTS

1. Industry Summary

Rootstock-induced dwarfing is a complex mechanism that causes a reduction in the size of the grafted scion by altering the floral and vegetative balance. Dwarfing rootstocks are essential to intensive production methods since they crop more and earlier. The impact of rootstock-induced dwarfing has previously been widely studied in scions but little is known about the role of dwarfing on root architecture. With the increase in food demand and climate change, it is essential to understand the impact of dwarfing on root architecture and how rootstocks can be optimised for both productivity and resilience to better adapt to future climate conditions.

Several QTL mapping studies have been conducted in apples to identify QTL linked to rootstock-induced dwarfing. However, the genetic basis of this complex trait remains unknown. A previous study which performed QTL mapping for root bark percentage, a trait associated with rootstock-induced dwarfing, identified three QTL named *Rb1*, *Rb2* and *Rb3* in Chromosomes 5, 11 and 13, respectively. In this thesis, fourteen SSR markers spanning *Rb1* and *Rb2* QTL were developed to fine-map these large QTL areas. The *Rb1* QTL region has been successfully reduced from 4.4 Mb to 2.2 Mb. Regarding *Rb2*, the analysis interestingly suggested that there were actually two QTL in that region, located between 6.9 Mb and 7.5 Mb, and between 10.9 Mb and 12.7 Mb. In addition, this thesis has generated useful markers linked to dwarfing that are currently used by breeders to accelerate the breeding process. Moreover, key genotypes have been generated during this study that will be useful to further fine map the dwarfing QTL.

Lastly, a selection of these rootstocks with different levels of dwarfing were collected from stoolbeds, grafted with Gala and planted in rhizotrons to analyse root system architecture changes over a season. It was found that dwarfing rootstocks exhibited a reduced maximum root system depth and convex hull area compared to vigorous rootstocks at the end of the first growing season. The great variability of data, especially in the dwarfing group, suggested that either dwarfing genotypes are more susceptible to environmental factors or that there are other genes influencing root architecture, opening the possibility of decoupling dwarfing and root system architecture. Furthermore, this study has also increased our knowledge about the methodology to evaluate root architecture in trees and how this could be improved to better explore tree root systems.

The findings of this research could also have a significant potential impact on other high-value perennial crops including cherry, pear and apricot since they are genetically related.

2. Introduction

2.1. Apple rootstocks

2.1.1. Benefits of the use of rootstocks

Rootstocks are defined as the part of the tree containing the root system and have been used in temperate fruit trees for more than 2000 years (Webster, 1995b). Rootstocks confer many characteristics to scions and have always been selected for a wide range of desirable traits such as pest and disease resistance, cold hardiness, good soil anchorage, reduced suckering as well as precocity and tree size (Pilcher *et al.*, 2008). Furthermore, tree root systems play a crucial role in nutrient uptake and adaptation to water deficit (Marguerit *et al.*, 2012). For all of these reasons, the choice of an appropriate rootstock is fundamental to orchard success.

With the increasing global demand for food, rootstock selection is gaining more importance since rootstocks with improved root systems can contribute to a better adaptation to drought periods and resistance to plant pathogens and therefore, impact yield (Jensen *et al.*, 2012; Marguerit *et al.*, 2012; Tamura, 2012).

2.1.2. Rootstock-induced dwarfing

Dwarfing rootstocks significantly impact the architecture and development of the scion. They reduce both the number and length of internodes, contribute to an early cessation of growth and a smaller trunk cross-sectional area, leading to an overall reduction of the tree size (Costes and Lauri, 1995; Atkinson and Else, 2001; Seleznyova *et al.*, 2003; Pilcher *et al.*, 2008). Furthermore, dwarfing rootstocks induce a higher proportion of buds to flower and precocity (Maggs, 1955; Webster, 1995a). For all of these reasons, dwarfing rootstocks are essential to intensive production methods since they contribute to a greater yield per unit area and crop more and earlier (Robinson, 2007). Rootstock-induced dwarfing is a complex trait influenced by several factors such as environmental conditions, growth parameters and scion variety. Many hypotheses have been proposed to explain dwarfing, most of them related to the altered root-to-shoot and shoot-to-root chemical signalling but the specific genes controlling this mechanism remain unknown.

2.1.3. Genetic control of rootstock-induced dwarfing in apples

Several studies have focused on performing quantitative trati loci (QTL) mapping analysis to identify genes controlling rootstock-induced dwarfing and to develop genetic markers closely linked to dwarfing that will help accelerate the breeding process. The first study conducted by Pilcher et al., (2008) genetically mapped *Dw1* in Chromosome (Chr) 5 using the progeny of a cross between the dwarfing rootstock 'M.9' and *Malus x Robusta 5* (R5) by measuring trunk cross-sectional area (TCSA), a measure for rootstock-induced dwarfing. Fazio et al., (2014) identified *Dw2*, a new dwarfing locus in Chr11 using a cross of Ottawa 3 x R5, with a similar effect on vigour. QTL for early bearing, rootstock height, tree height, fruit count and flower density were found to roughly colocalize with *Dw1* and *Dw2* QTL (Fazio *et al.*, 2014). A later study using another M.9 x R5 population identified two major QTL. *Dw1* was found to colocalise with the previously published location but *Dw2,* although it was also situated in Chr11, it was placed in a slightly different location than the one reported by Fazio et al., (2014) (Foster *et al.*, 2015). A high proportion of root bark (cortical cells) in the apple rootstock has been previously associated with rootstock-induced dwarfing (Beakbane and Thompson, 1947). In 2016, a QTL map for root bark ratio, a primary trait related to dwarfing, was performed using the progeny of a cross of M.27 x M.116 (M432 population) and identified *Rb1* and *Rb2* which colocalized regions previously associated with dwarfing (Harrison *et al.*, 2016). *Rb1* colocalized with the region identified as controlling dwarfing in Chr5 (Pilcher *et al.*, 2008; Fazio *et al.*, 2014; Foster *et al.*, 2015) and Rb2 was situated in the same area as the *Dw2* identified by (Foster *et al.*, 2015). Furthermore, Harrison et al., (2016) discovered a third QTL, *Rb3*, located in Chr13.

2.2. Root architecture

Root system architecture (RSA) can be described as the spatial distribution of roots (Lynch, 1995; Osmont *et al.*, 2007). RSA contributes to plant hydraulics, anchorage and nutrient uptake (Bohn *et al.*, 2006; Lynch, 2007; Paez-Garcia *et al.*, 2015; Ludlow and Muchow, 1990). Root systems have great plasticity and root development is modified by a wide range of factors including genetics, soil environment and resource availability (van der Weele *et al.*, 2000; López-Bucio *et al.*, 2003; Hodge, 2004; Malamy, 2005; Koevoets *et al.*, 2016; Karlova *et al.*, 2021).

2.2.1. The impact of dwarfing rootstocks on root system architecture

Extensive research has been conducted on how rootstock-induced dwarfing affects apple scions, but there has been relatively limited exploration into the consequences of dwarfing on root systems. Some studies have shown that the root systems of dwarfing rootstocks had a reduced root spread area with lower total root density and thinner roots while vigorous rootstocks displayed deeper root systems with higher total root density (De Silva, 1999; Lo Bianco *et al.*, 2003; García-Villanueva *et al.*, 2004; Hou *et al.*, 2012; An *et al.*, 2017b).

In summary, vigorous rootstocks demonstrate better root growth and adaptability to drought while dwarfing rootstocks are poorly anchored to the soil and are more sensitive to environmental stresses due to smaller root systems (Tworkoski and Fazio, 2015).

2.3. Challenges in understanding rootstock-induced dwarfing, root system architecture and breeding for resilience: Knowledge gaps

The impact of dwarfing on scions has been a well-explored subject, yet the underlying genetic basis remains unknown. Three QTL associated with rootstock-induced dwarfing have been identified in apple (Harrison et al., 2016) although the areas covered by these QTL are quite large and contain hundreds of candidate genes. One of the objectives of this study is to fine-map the dwarfing QTL to narrow down the regions and identify the genes controlling this complex mechanism. Furthermore, breeding dwarfing rootstocks is complicated since the dwarfing effect is usually lost over generations, therefore new molecular markers strongly linked to rootstock-induced dwarfing are essential to hasten the breeding process. Here I aimed to generate genetic markers associated with dwarfing that could help breeders accelerate the breeding process of new dwarfing rootstocks.

Moreover, there has been limited research on the impact of dwarfing on the root system architecture of apples. Another aim of this project was to investigate how dwarfing influenced root traits such as total root length, maximum root depth or convex hull area that could be desirable for breeding deep-rooted rootstocks since this will improve soil anchorage and adaptability to different climate conditions. This research will help to elucidate if rootstock-

induced dwarfing and root system architecture can be decoupled to generate new rootstocks with improved root systems while maintaining the advantages of dwarfing. The end goal is to better understand the genetic and biological processes associated with rootstock-induced dwarfing and obtain markers closely linked to dwarfing and root traits that will aid the generation of more resilient rootstocks while keeping all the benefits of dwarfing.

3. Materials and methods

3.1. Fine mapping the root bark QTL associated with rootstock- induced dwarfing

3.1.1. Primer development and identification of dwarfing alleles

Single Sequence Repeat (SSR) detection

In preparation for this project, M.9, M.M.106, M.27, M.13 and M.116 rootstock genomes were sequenced using the Illumina HiSeq 2000 platform. In order to identify Single Sequence Repeats (SSRs) in the root bark QTL regions associated with roostock-induced dwarfing (Harrison et al., 2016) (Figure 1), the sequenced rootstocks were piled up and variant calling was performed using Samtools version 1.5 (Li *et al.*, 2009).

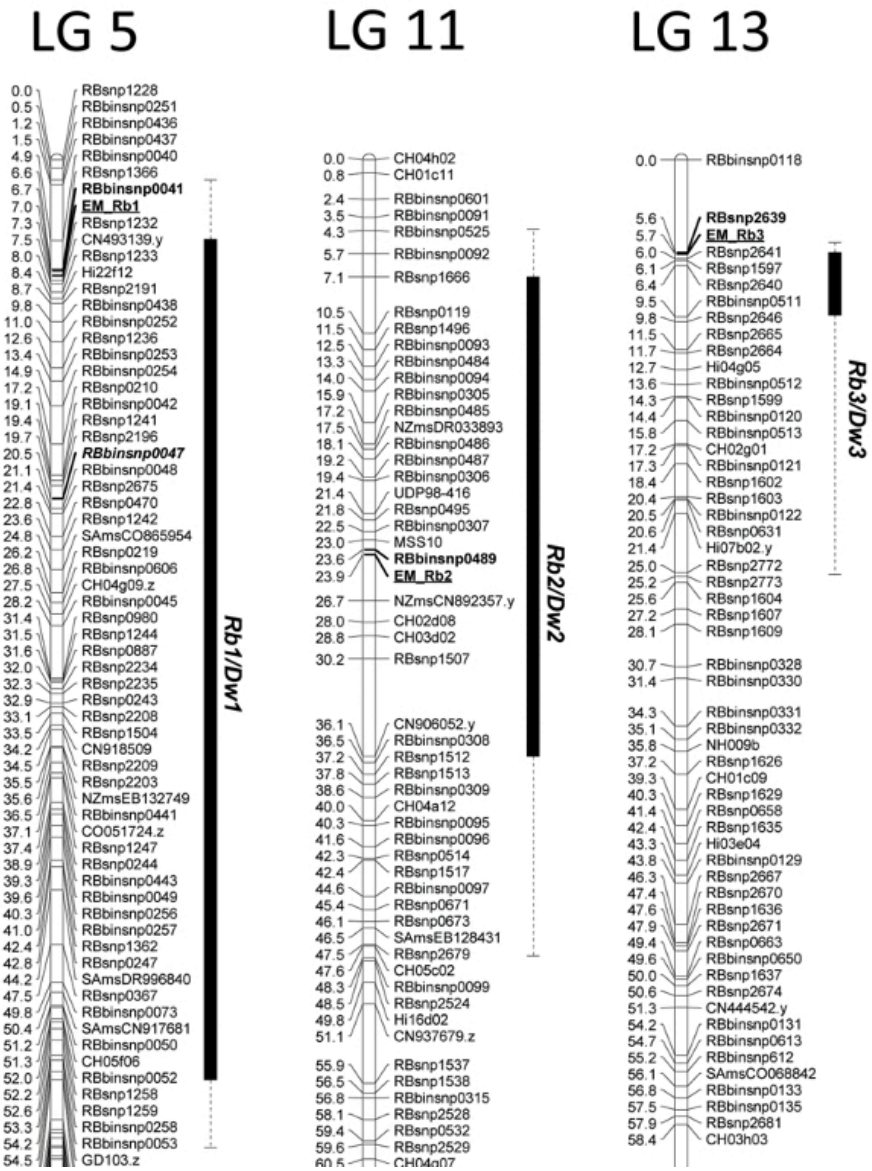

Figure 1. Root bark percentage QTL map using M432 population (M.27 x M.116). Markers found to be most significantly linked by (Harrison et al., 2016) are shown in bold.

Primer design

Highly polymorphic SSRs along the regions in Chromosomes 5 and 11 were selected as a target for primer design using Primer3 software (Untergasser *et al.*, 2012) available in Geneious. The M13-tailed primer method (Boutin-Ganache *et al.*, 2001) was used to label amplicons for visualization after capillary electrophoresis on a 3130xl genetic analyser (Applied Biosystems). Forward primers were 5'-tailed with the 18bp M13 tail (TGTAAAACGACGGCCAGT). The M13-tailed primer was 5'-fluorescently tagged with 6-FAM, HEX, NED or PET to facilitate multiplexing.

DNA extraction, PCR amplification and DNA genotyping by capillary electrophoresis

Leaf samples were collected from M.9, M.27, M.26, M.116 and M.M.106 rootstocks for further DNA extraction. The method chosen for the DNA extraction was Silica Bead Method described in (Edge-Garza *et al.*, 2014).

DNA from the rootstocks mentioned above was used to test all the primers. The polymerase chain reaction (PCR) was conducted in 13 µl reactions containing 10 ng of gDNA, 1.25 µl of forward primer (2 µM), 1.25 µl of reverse primer (2 µM), 1.25 µl of the dye (2 µM), 6.25 µl of Type-it Multiplex PCR Master Mix from Qiagen and 1 µl of water. Diverse thermal profiles were tested on the primers during the optimisation process. The following touchdown PCR programme was used for all of them since this produced the best results: 95°C for 5 minutes followed by 10 cycles of 95°C for 30 seconds, then 57°C for 90 seconds and 72°C for 45 seconds (annealing temperature was gradually reduced by 0.5°C every cycle). The PCR reaction was continued with 20 cycles of 95°C for 30 seconds, then 52°C for 90 seconds and 72°C for 45 seconds. The reaction was finished with a final elongation step at 60°C for 30 minutes.

PCR products tagged with different dyes were pooled and diluted 1 to 10 with distilled water. The ABI PRISM 3130*xl* Genetic Analyzer was used to determine the exact size of the PCR fragments. Sample preparation for capillary electrophoresis consisted of a mixture of 1.3 µl of PCR dilution plus 9 µl of the electrophoresis mix (8.75 µl of deionized formamide and 0.25 µl of GeneScan(™) 500LIZ(™) from Applied Biosystems). The sample mix was denatured for 3 minutes at 90°C and cooled on ice prior to loading the instrument. Amplicon size analysis was executed using the recommended software, GeneScan version 3.7 and Genotyper version 3.7.

Dwarfing allele identification using the M432 population

The more polymorphic and easier-to-score SSR markers were selected and tested on germplasm of known phenotype to identify the dwarfing allele(s). DNA from 18 individuals from a previously characterised mapping population (M.27 x M.116 cross) was used. The selected individuals did not show any recombination events in the areas of interest. This population had been previously used for the detection of QTL controlling the root bark ratio

(Harrison et al., 2016), therefore, genotypic and phenotypic information from each individual was available.

In order to identify the alleles linked to dwarfing from markers in Chr5, genotypes with high root bark percentage (above 80%) and presenting the SNPs associated with the root bark QTL were selected as an unequivocal dwarfing cohort. In addition, genotypes that did not show the SNPs associated with root bark QTL and with a small root bark percentage were selected as vigorous controls. Primers were tested on these individuals following the same PCR protocol and amplicon analysis as described in the previous section.

3.1.2. Plant material

Seven crosses between interrelated rootstocks with well-characterised effects on scion vigour were made in preparation for this project (MCM families). Seeds were collected and germinated and trees were planted in pots and placed in a polytunnel for further phenotyping (Table 1).

Table 1. Parentage, number of seeds sown, seed germinated and surviving trees of the MCM rootstock populations.

Family name	Female	Male	Seeds sown	Seeds germinated	Surviving trees
MCM001	M.9	M.27	150	56	42
MCM002	M.27	M.26	224	117	98
MCM003	M.116	M.27	398	227	184
MCM004	M.27	M.116	184	48	38
MCM005	M.9	M.26	143	52	34
MCM006	M.26	M.27	263	157	140
MCM007	M.M.106	M.27	697	424	335
Total			2059	1081	871

In addition, four apple rootstock trial plots that had been evaluated as part of the East Malling Rootstock Club were excavated using a digger. All the rootstocks in these trials had a dwarfing parent or grandparent; therefore, the dwarfing haplotype(s) could be present in them and their characterisation could contribute to the fine mapping of the root bark QTL (Supplementary Table S1).

DNA from the MCM families was extracted using Silica Bead Method described in (Edge-Garza *et al.*, 2014) DNA from the rootstocks located in the trials was available after being extracted by members of the rootstock breeding team at NIAB EMR.

3.1.3. Plant phenotyping

In December 2019, height and trunk diameter were measured in the 357 trees that actually belonged to the MCM crosses and were still alive. Three to ten root segments (2–8 mm in diameter, 50–80 mm in length) were excised from each root system using secateurs, placed into a labelled polythene bag and stored at 4°C before analysis. Each root root fragment was carefully washed using tap water and a scalpel or knife was used to remove a ring of bark (cortex) approximately 2–3 mm in length, leaving behind the stele of the root (Figure 2). Digital callipers were used to make pairs of measurements of the root with and without the bark. For each root, the cross-sectional area of the root was calculated as well as the percentage of the total area occupied by the root bark, assuming that the root section was a perfect cylinder.

Figure 2. Root segments after removing a ring of bark. Green arrow pointing to the area where the stele of the root remains.

The exact number of rootstocks sampled in each trial is detailed in Supplementary Table S1. Between six and twenty root segments (4–10 mm in diameter, 80–120 mm in length) were excised from each root system using secateurs, placed into a labelled polythene bag and stored at 4°C before analysis. The roots were measured following the same protocol previously described.

3.1.4. Primer selection and screening

First batch of primers

Eight SSR markers were screened at the same time in the ABI PRISM 3130*xl* Genetic Analyzer to allow for allele variation in previously untested material. In order to multiplex eight primers, four dyes and primers with small and large amplicon sizes in each dye were used. In this screening, only markers in Chromosomes 5 and 11 were used since the QTL on these regions have a major effect on dwarfing. More markers were needed to characterise the Chr5 region since this is an area of low recombination with few polymorphic SSRs for which primers of suitable amplicon size could be designed.

Five loci were selected spanning the whole region in Chr5 and three loci were used to cover the whole length of the dwarfing region in Chr11. Primers for the eight loci were ordered with the forward 5'-fluorescently labelled with different dyes (6-FAM, HEX, NED and PET). Each dye was attached to two different primers and dyes were assigned ensuring that within each dye, amplicon sizes did not overlap.

The eight primers detailed in Table 2 were mixed and diluted to a final 2 µM concentration and multiplexed in one PCR reaction. The PCR reaction was conducted in 13 µl reactions containing 10 ng of gDNA, 1.25 µl of multiplexed primers (2 µM), 6.25 µl of Type it and 3.5 µl of water. The following touchdown PCR programme was used: 95°C for 5 minutes followed by 10 cycles of 95°C for 30 seconds, then 55°C for 90 seconds and 72°C for 30 seconds (annealing temperature was gradually reduced by 0.5°C every cycle). The PCR reaction was continued with 20 cycles of 95°C for 30 seconds, then 50°C for 90 seconds and 72°C for 30 seconds, and a final elongation step at 60°C for 30 minutes. Sample preparation for capillary electrophoresis and amplicon size analysis was performed as previously detailed.

Table 2. Genome positions, primer sequences, amplicon range (in MCM families), repeat motif, fluorescent dye and multiplex for PCR for the first eight SSR markers used to genotype the MCM rootstock populations.

Marker Name	Chr	Marker position in GD (bp)	Forward primer sequence 5'>3'	Reverse primer sequence 5'>3'	Amplicon size range (bp)	Motif	Dye	Multiplex
CH03a09*	5	41424461	GCCAGGTGTGACTCCTTCTC	CTGCAGCTGCTGAAACTGG	127-131	AG	FAM	Small
MD5002	5	41992706	AACATCGTGCCATGGATCCG	ACCACCATTGTTGCTTGCAA	203-229	AT	HEX	Large
MD5003	5	42191842	ACCTCCAATGCTGAGCTGAA	CCGCCAGCATGCATTTCATT	140-163	AG	HEX	Small
MD5004	5	45680011	TGGGAACTATCTTGTTTCGACT	AGGGTGGGAAACACTTGCTT	249-253	TG	NED	Large
MD5005	5	45829539	GCCGATTGATTTTCCTCTTCCA	GCGTGACTCCCTCTCATTGG	185-203	AG	NED	Small
MD11001	11	6967726	CGGAAATGTCAAATTCGCAACC	TAGCGACTTGTGTGTGTGGG	197-220	AT	PET	Large
MD11002**	11	9834270	CTTTCCCTTTTGCCACCACC	GCAGACACTCACTCACTATCTCTC	140-184	GA	PET	Small
MD11003	11	12737959	GCTCATTTTCTTCTTAAGCAGCC	CCAGTTCCTTACCAAGCAAAATGT	268-278	AT	FAM	Large

* CH03a09 has been already associated with rootstock-induced dwarfing (Pilcher *et al.*, 2008).
** MD11002 amplifies the same locus as the CH02d08 marker that has been previously associated with dwarfing (Fazio *et al.*, 2014) but new primers for this marker have been developed to meet the amplicon size requirements for multiplexing. Original sequences in (Liebhard *et al.*, 2002)

Second batch of primers

The first batch of markers was screened on the seven rootstock populations to identify recombinant genotypes. Additional markers were subsequently tested to have as much marker coverage of the QTL regions to detect recombination points. This section summarises this new batch of primers.

Primer pairs for six new markers were ordered with the forward 5'-fluorescently labelled with two different dyes (6-FAM and HEX) and PCR was performed as described in the previous section. Two multiplexes were prepared, one to amplify the two new loci in Chr5 (MCM5006 and MCM5007) and another to amplify the four new loci in Chr11 (MCM11004, MCM11005, MCM11006 and MCM11007) (Table 3). The allele(s) linked to dwarfing for these markers were identified following the same procedure previously described as well as PCR conditions, capillary electrophoresis and amplicon analysis.

Table 3. Genome positions, primer sequences, amplicon range (in MCM families), repeat motif, fluorescent dye and multiplex for PCR for the second batch of SSR markers used to genotype the MCM rootstock populations.

Marker Name	Chr	Marker position in GD (Mb)	Forward primer sequence 5'>3'	Reverse primer sequence 5'>3'	Amplicon size range (bp)	Motif	Dye
MD5006	5	43035949	CCTTCACTTCCTGCCCATCC	GTCGTGGATGCTTTACCCCA	235-247	GA	FAM
MD5007	5	45229790	TGACAGCTCAGCAGTTCTCTG	ACAGCAGGCATTGTTAGGGT	262-296	CT	HEX
MD11004	11	7584542	CCCACTTCTGCTGCACTACA	AGGGGCGTTTTGATATGGGG	191-203	TA	HEX
MD11005	11	8339391	TCACTGGTGGTTCTCGATCG	CGTCGCGTACTCTGATGTCA	116-128	TA	FAM
MD11006	11	10423899	GTTTGTTGTGAAGTGAGTCCCT	TTCGATGTAATGTGGACCCCA	164-177	GT	FAM
MD11007	11	10926735	TGAAATTTTCCGACGAACCTGA	TCGCATCGCCTTCTTCTCTC	153-161	GA	HEX

Data analysis

The allele information obtained after genotyping the rootstocks using the markers developed was phased to obtain the tentative haplotypes of each individual. The phasing of haplotypes refers to the process of determining the specific combination of alleles on each of the two homologous chromosomes in an individual's genome. The most likely distribution of alleles was annotated for each haplotype in an Excel document for all the individuals in each cross. The identification of haplotypes will help to detect recombinants by comparing them with the dwarfing haplotype initially identified to better determine the position of the QTL (fine mapping).

Recombinant genotypes are missing a part of the tentative dwarfing haplotype. If they still present the dwarfing phenotype, this would indicate that the region lost during that particular recombination does not contain the dwarfing gene. Conversely, a loss of the phenotypic expression would indicate that the gene responsible for that dwarfing QTL is located within that lost region. Since both, *Rb1* and *Rb2* are needed to cause dwarfing, while evaluating the effect of a recombination at one locus, the other locus always contained a full copy of the dwarfing haplotype with no recombinations.

The root bark percentage of each genotype was calculated by estimating the root bark percentage of a 7.5 mm diameter root using regression analysis. The genotypic information together with the phenotypic information was used to evaluate if the lost of part of the dwarfing haplotype affected or not the phenotype.

3.2. Effect of dwarfing on root architecture in apple rootstocks

3.2.1. Genotyping

The MDX132 family is the progeny of a Golden Delicious (GD) x M.9 cross; 287 seedlings were planted in a ‘Deadmans Field’ plot at NIAB EMR (Kent, UK) in 2016. DNA from 148 individuals of the MDX132 mapping population and the parents (GD and M.9) was extracted using the Qiagen DNeasy Kit. The Illumina Infinium® SNP array (also known as the 20K array) was used for genotyping the 150 individuals. DNA was prepared according to the manufacturer's recommendations.

3.2.2. Lifting stoolbeds and rooting phenotyping in 2020

The MDX132 population was planted as stoolbeds. Rootstocks were stooled in June 2018 to conduct the experiment in 2019 but unfortunately, not many genotypes produced well-rooted shoots and, therefore, the experiment was postponed until 2020. In January 2020, stoolbeds were carefully unearthed and rooted shoots were labelled and stored at 4°C for further experiments on root system architecture.

3.2.3. Genotype selection for root architecture experiment

SNPs flanking *Rb1* and *Rb2* QTL regions were identified and individuals with no recombinations in these areas were classified into four groups, depending on the presence or absence of the haplotypes linked to *Rb*1 and *Rb2* respectively. Although both QTL regions are needed to cause dwarfing, groups with only one of the RB QTL were also included to determine what, if any, individual effect each QTL had on root traits. A total of 39 genotypes with no recombination were included in this experiment (Table 4).

Table 4. Number of genotypes in each dwarfing class based on the presence or absence of the *Rb1* and *Rb2* QTL and the predicted vigour

***Rb1* haplotype**	***Rb2* haplotype**	**Number of genotypes**	**Predicted vigour**
No	No	9	Vigorous
Yes	No	10	Vigorous
No	Yes	8	Vigorous
Yes	Yes	12	Dwarfing

3.2.4. Root system architecture rhizoboxes

Non-recombinant a genotypes selected for this experiment were grafted at the end of March using Gala graft wood collected from a single Gala tree available at the NIAB EMR. Afterward, grafted trees were planted in rhizoboxes (100 cm x 30 cm x 3 cm) filled with sieved standard compost without slow-release fertilizer to avoid interference with the

imaging since the whitish colour of the fertiliser can be confused with roots during image processing. Rhizoboxes were covered with white reflective plastic to prevent roots from direct light. The rhizoboxes were randomised in 4 blocks and placed in a glasshouse compartment at an inclination of approximately 15° (Figure 3. Panel A). Trees were fertigated twice a day for 2 minutes at 8 am and 4 pm using a Dosatron with Universol Green 23-6-10 (N-P-K) fertiliser.

3.2.5. Canopy phenotyping and imaging

Rhizobox imaging and canopy phenotyping (data not shown) took place every six weeks from June until October 2020. A homemade imaging rig was set up with 2 Canon 1200D cameras with an 18-55 mm telephoto (using the 18 mm) on a camera slider. The total length of the rhizobox was covered by overlapping the two images. The imaging platform consisted of a Dexion frame where the rhizoboxes were positioned at a fixed distance from the camera. The whole imaging structure was covered by a black cloth and two Manfrotto LED lighting units were used to minimise the variation of the ambient light as much as possible. Images were taken at an f stop of 5.6 to 6.3 at 1/60 using a shutter release (Figure 3. Panel B).

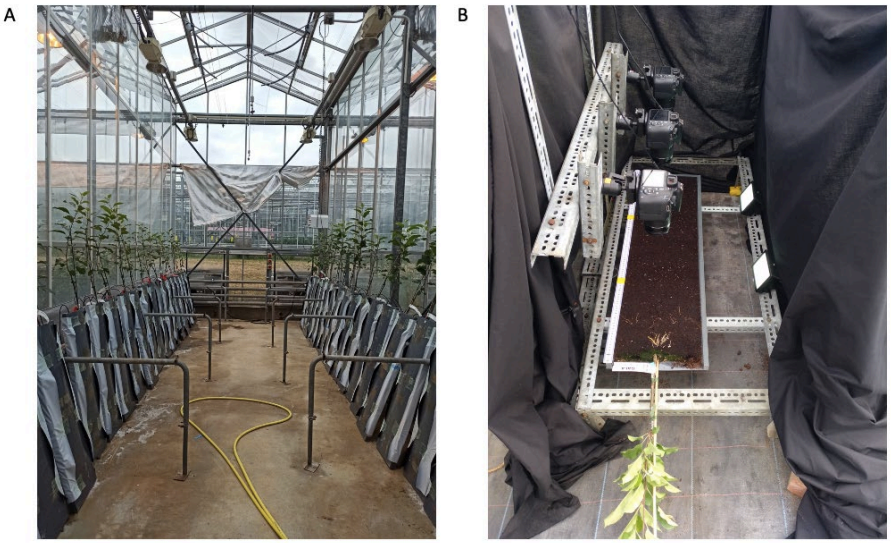

Figure 3. Details of the root system architecture experiment. A: Rhizoboxes in the glasshouse compartment. B: Custom-made imaging rig used for root systems phenotyping.

3.2.6. Imaging analysis

Chromatic aberrations and lens distortion were corrected using the RawTherapee imaging analysis software version 5.8 (RawTherapee 5.8, 2020). Then, the two photos of each rhizobox were stitched together using the Fiji plug-in available in ImageJ 2.1.0 (Schindelin *et al.*, 2012). Differences in the contrast between the two images were adjusted and a composite image of the rhizobox was created using the montage option and the least square mode. The photos were then exported in PNG format at the best resolution. Afterward, the composite images were reopened using Fiji and the region containing the root information was cropped avoiding the rhizoboxes edges.

Image segmentation, cleaning, re-cropping and root measurements were done using Python scripts developed by Ben Pennington while working at NIAB EMR in 2016 using Python 2.7 (van Rossum, 1995) and that I adapted it to this experiment. In the segmentation script, the photo was converted into a white and black image where the roots were transformed into white pixels and the soil into black pixels. In this script, the number of clusters used to segment the images ranged from 4 to 7. In general, this script worked well using 5 clusters (4 images detecting soil and 1 image for roots). When not completely satisfied with the segmentation of the images, the number of clusters was increased. Occasionally, not all the roots appear clearly in one segmented image. In this case, GIMP version 2.10 (GNU Image Manipulation Programme, 2020) software was used to combine both images to obtain the whole root system in one picture. The segmented images were then cleaned using a cleaning script that removed small blobs of pixels, also known as background noise, that could be mistakenly identified as roots. The size of the blobs was modified in the script depending on how much noise there was in each image. Each image was carefully reviewed and re-cleaned manually using ImageJ if needed. Next, the re-cropping script was used to remove regions of the rhizobox image that contained imaging artefacts.

Finally, the measurement script was utilised to generate an Excel table containing several root measurements such as total root length, maximum root system depth and convex hull area. Graphical outputs were also produced for each image such as the root diameter distribution of each rhizobox, convex hull figures and skeleton photos (Figures 4 and 5).

3.2.7. Statistical analysis

Linear mixed models fitted by REML were used for the root traits data analysis including total root length, root system depth and convex hull area using the “lme4” package available in R (Bates *et al.*, 2015). The model selection was performed by dropping variables and comparing models with likelihood ratio tests using the ANOVA function. The best consensus model was chosen for all the analyses. The final model consisted of eight fixed variables: block, time point (TP), *Rb1*, *Rb2*, all the possible interactions of TP, *Rb1* and *Rb2* and genotype as a random variable. Post hoc contrasts were performed using the “emmeans” package available in R (Lenth *et al.*, 2018). Total root length was transformed using the square root transformation to improve the distribution of the residuals. Graphical outputs were obtained using the “ggplot2” (Wickham, 2016) and the significance letters were added creating compact letter displays (CLD) of all pairwise comparisons using the “multcomp” and “multcompView” packages available in R (Hothorn *et al.*, 2008; Graves *et al.*, 2019).

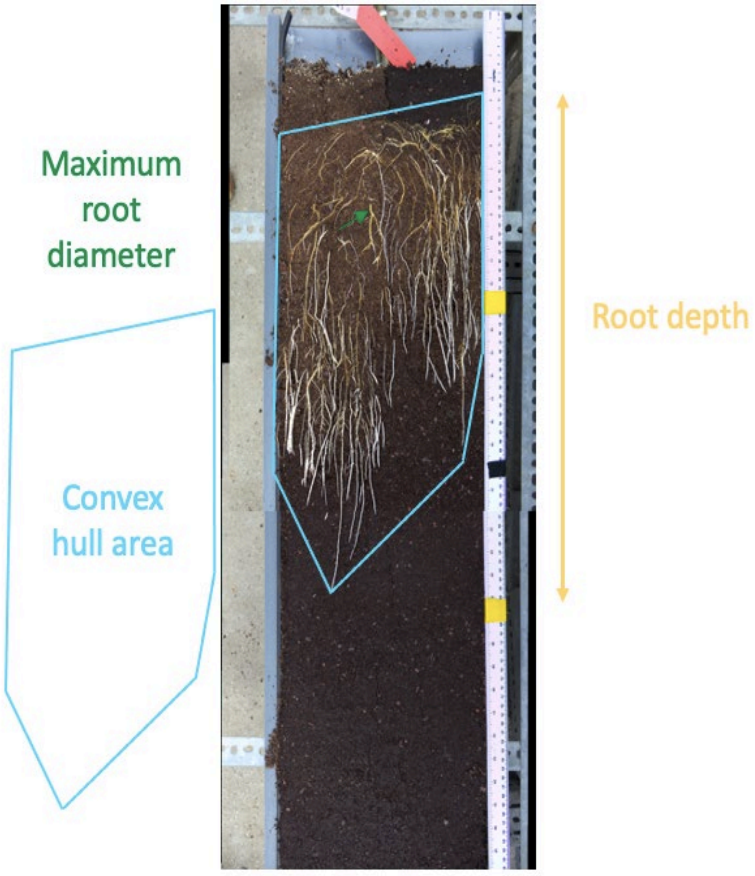

Figure 4. Diagram representing some of the root measurements taken from apple rootstocks grown in rhizoboxes.

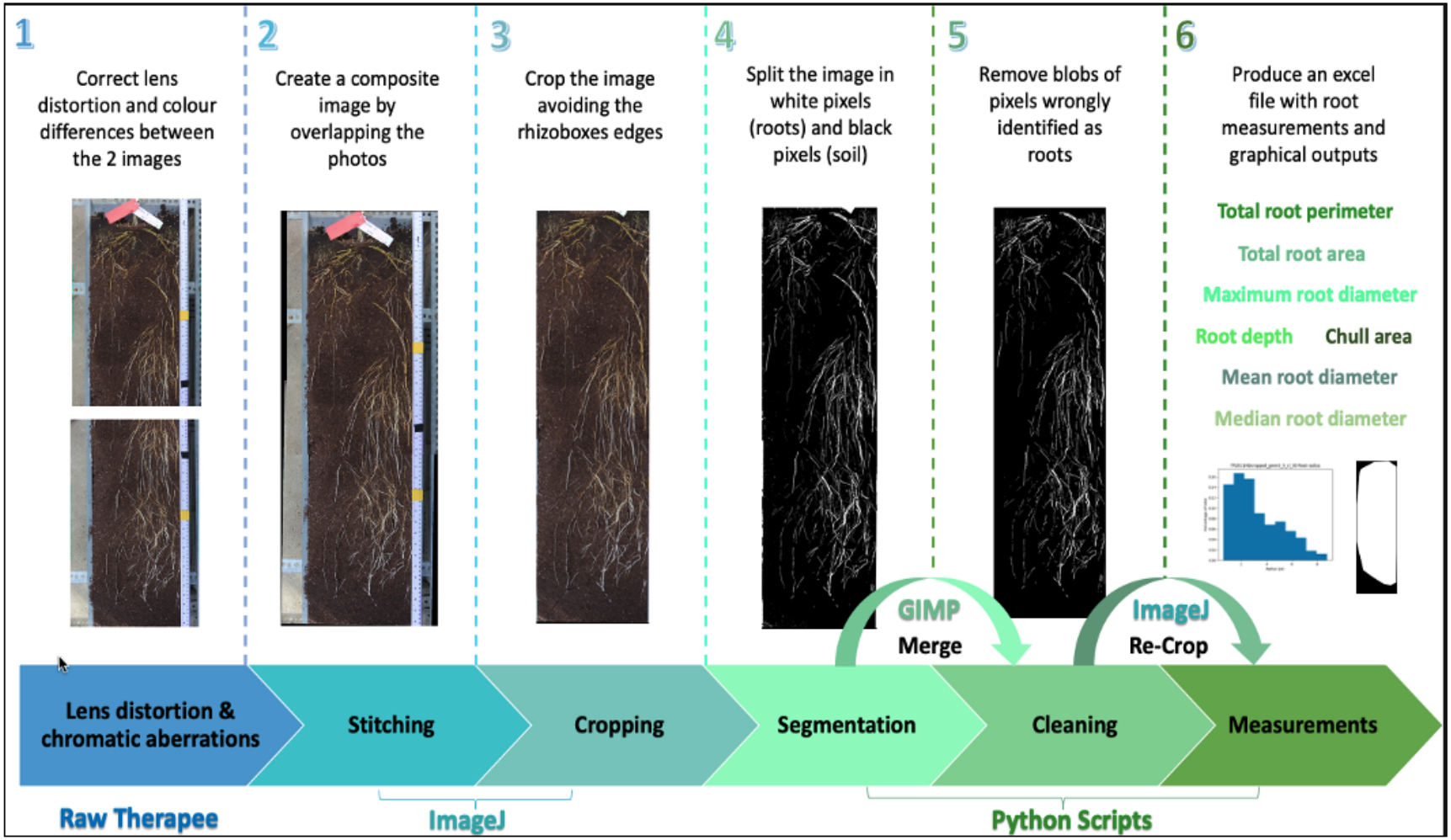

Figure 5. The imaging analysis pipeline detailing the steps and programs used during the imaging analysis of the root architecture traits in the MDX132 population (GD x M.9 cross).

4. Results

4.1. Fine mapping of the root bark QTL

4.1.1. Identification of dwarfing haplotypes

The dwarfing haplotype was determined in the parents of the MCM crosses as well as in the parents of the selections available in the trials (whenever possible) so that recombinant genotypes could be identified (Figure 6).

	M.27		M.26		M.116		M.M.106		M.9	
Markers Chr5	H1	H2	H1	H2	H1	H2	H1	H2	H1	H2
CH03a09	132	130	132	132	132	130	132	128	132	128
MD5002	204	208	204	204	202	208	202	200	204	null
MD5003	141	162	141	141	150	162	150	138	141	150
MD5006	235	245	235	235	247	245	247	245	235	247
MD5007	286	264	276	262	279	266	279	296	276	286
MD5004	248	252	250	250	250	252	250	250	250	248
	M.27		M.26		M.116		M.M.106		M.9	
Markers Chr11	H1	H2	H1	H2	H1	H2	H1	H2	H1	H2
MD11001	212	197	212	197	212	204	204	220	212	220
MD11004	203	191	203	191	203	null	null	199	203	199
MD11005	128	116	128	116	128	null	null	99	128	124
MD11002	142	155	142	155	142	140	159	140	142	142
MD11006	164	170	164	168	164	170	177	170	164	168
MD11007	159	153	159	157	159	155	161	155	159	161
MD11003	272	276	272	266	272	268	266	268	272	278

Figure 6. Estimated haplotypes in the parents of MCM families showing allele sizes for all the markers used in this study. Highlighted in blue, the dwarfing haplotype. In red, allele sizes that are similar to the alleles associated with dwarfing.

All the markers used in M.26 are homozygous except one, making it almost impossible to distinguish which haplotype is dwarfing in crosses with M.26 as a parent. Furthermore, the amplification of the MD5005 primer was poor in several seedlings from all crosses so this marker was excluded from the analysis for consistency. Since this marker was

outside the tighter QTL region identified in this study, we did not aim to replace it or redesign the primers (Figure 6).

4.1.2. Recombinant genotypes

Once the dwarfing haplotypes were identified in the parents of the MCM crosses, the selections available in the breeding trials and their parents, genotypes with key recombinations in areas of interest were examined.

Figure 7 shows the allele sizes of genotype 131 from the MCM007 family (M.M.106 x M.27 cross). The haplotype 2 from MCM007-131 is the result of a recombination event in M.27 and, therefore, MCM007-131 inherited the dwarfing alleles only for markers MD11007 and MD11003. The root bark percentage of MCM007-131 was 68.8 %, measuring 98 cm in height and the trunk diameter measured 6.77 mm. In summary, MCM007-131 genotype conserved the dwarfing phenotype despite losing part of the dwarfing haplotype in Rb2 area, indicating that the genes responsible for dwarfing should be located between MD11007 and MD11003 markers. A similar analysis was done for each recombinant to narrow down the root bark QTL areas.

	M.M.106		M.27		MCM007-131	
Markers Chr5	**H1**	**H2**	**H1**	**H2**	**H1**	**H2**
CH03a09	132	128	132	130	128	132
MD5002	202	200	204	208	200	204
MD5003	150	138	141	162	138	141
MD5006	247	245	235	245	245	235
MD5007	279	296	286	264	296	286
MD5004	250	250	248	252	250	248
Markers Chr11	**H1**	**H2**	**H1**	**H2**	**H1**	**H2**
MD11001	204	220	212	197	204	197
MD11004	null	199	203	191	null	191
MD11005	null	99	128	116	null	116
MD11002	159	140	142	155	159	155
MD11006	177	170	164	170	177	170
MD11007	161	155	159	153	161	159
MD11003	266	268	272	276	266	272

Figure 7. Estimated haplotypes of MCM007-131 and its parents showing allele sizes for all the markers used in this study. Highlighted in blue, the dwarfing haplotype. Thick line indicates the recombination point.

4.1.3. Fine mapping of *Rb1* and *Rb2*

Once all the genotypes with recombinations were analysed, *Rb1* and *Rb2* QTL were fine mapped. *Rb1* region that originally covered approximately 4.4 Mb was narrowed down to 2.2 Mb and therefore, the gene located in this region would be situated between MD5006 and MD5007 markers. Regarding *Rb2*, the analysis interestingly suggested that there were actually two QTL in that region, located between 6.9 Mb and 7.5 Mb, and between 10.9 Mb and 12.7 Mb (Figure 8).

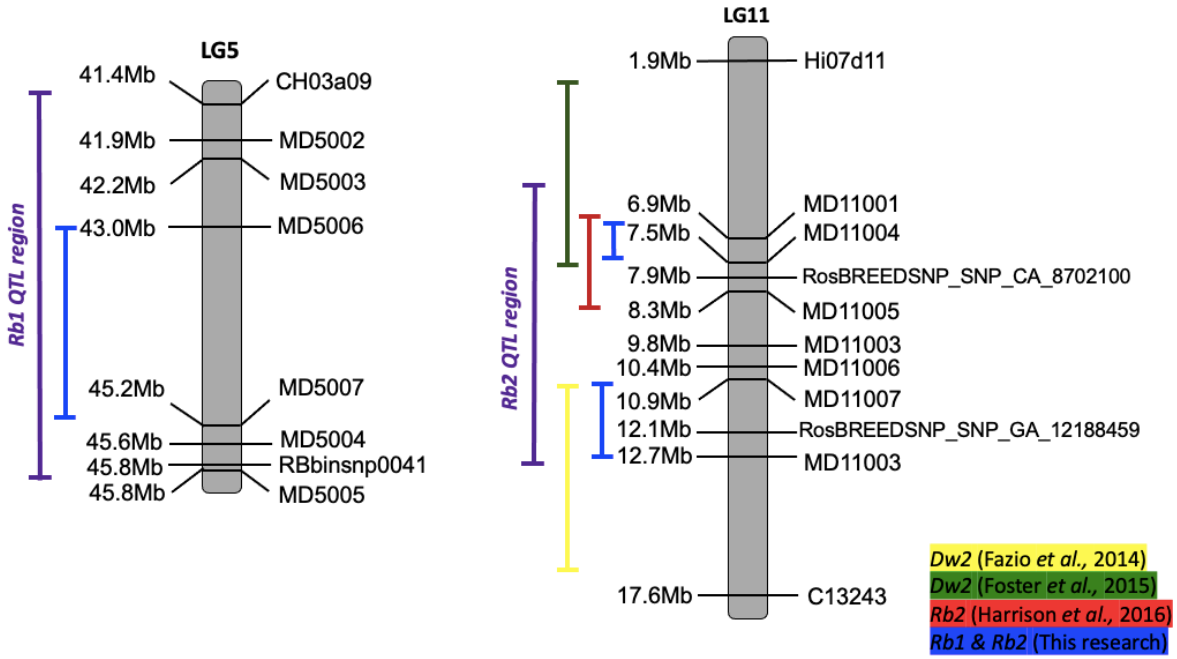

Figure 8. Diagram showing *Rb1* and *Rb2* QTL regions before and after fine mapping and the approximate location of *Dw2/Rb2* according to different authors.

4.2. Effect of root bark (RB) QTL on root traits

Rootstock breeding has focused extensively on how dwarfing affects the scion, but there is limited knowledge of how it affects root systems. To gain a better understanding of the impact of this complex trait on apple trees, this study assessed how rootstock-induced dwarfing affects critical root system traits. The effect of *Rb1* and *Rb2* on the root traits was analysed using REML analysis.

4.2.1. Effect of RB QTL on total root length (TRL)

For the analysis of TRL, time point was the only significant variable in the model (p-value = <2e-16). This is not surprising since the TRL increases over time (Table 5). Emmeans was used to get the model estimated (marginal) means and contrast p-values within each time point. No significant differences between the groups were identified. The mean of the *Rb1Rb2* group was consistently lower than the mean of the other groups from TP2.

Additionally, the differences between groups became more evident over time. In TP4, the comparison between NoRb and *Rb1Rb2* groups was close to being significant (p-value=0.06). This suggests that if the experiment had been conducted for a longer duration, there might have been noticeable variations among the dwarfing categories in terms of TRL (Figure 9 and Supplementary Tables S2 and S3).

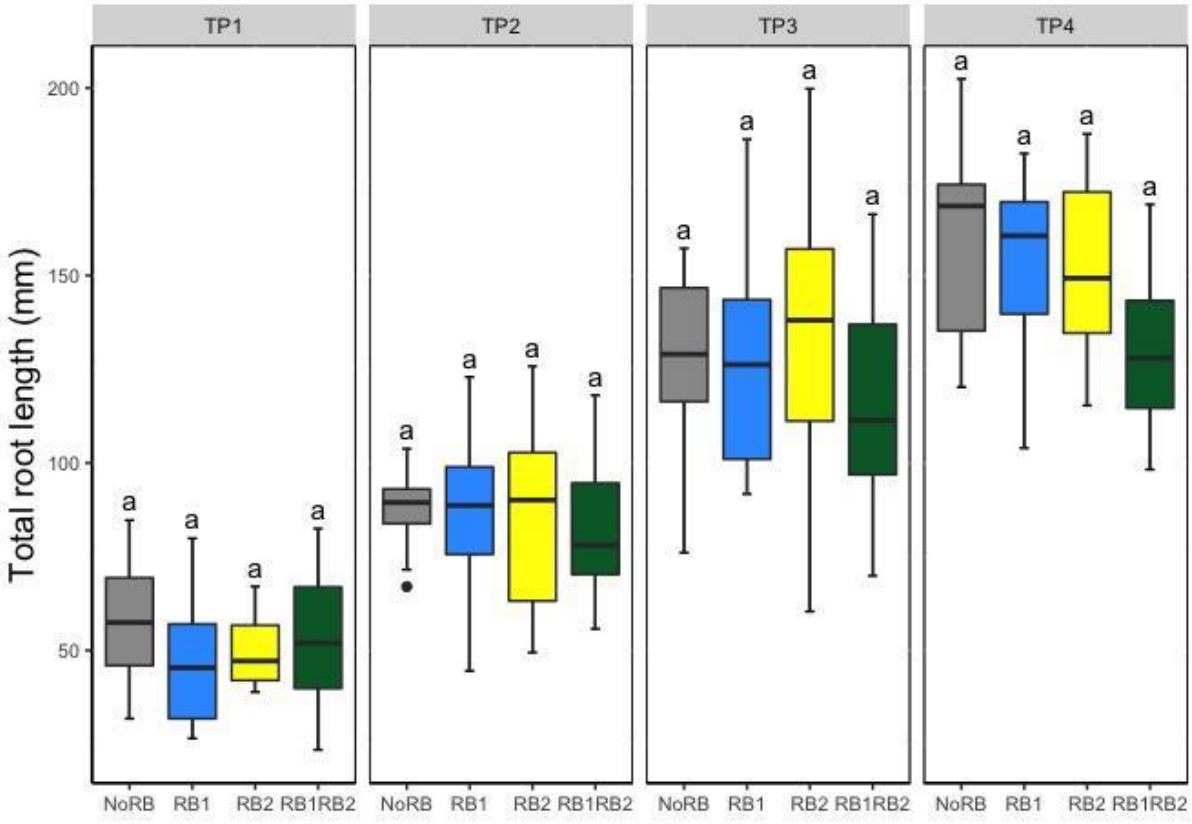

Figure 9. Total root length (square transformed) of grafted rootstocks with different combinations of root bark QTL per time point. Centerlines show the medians; whiskers mark the maximum and minimum values, respectively. Upper and lower box boundaries represent the 25th and 75th percentiles, respectively. Different lower-case letters are significantly different ($p<0.05$).

4.2.2. Effect of RB QTL on the total root system depth

The analysis of maximum root system depth area in the apple rootstocks showed that time point, block, and the interaction between *Rb1* x TP were all statistically significant (p-value < 2.2e-16, 4.329e-05 and 0.004, respectively) and therefore, had an effect on root depth (Table 5).

Despite the fact that *Rb1* and *Rb2* were not significant in the model, comparisons between dwarfing classes were performed within each time point and significant differences between dwarfing groups appeared in TP3. Differences between NoRb and *Rb1Rb2* groups were observed (p-value = 0.0028) and also when comparing *Rb2* and *Rb1Rb2* (p-value = 0.0053; Supplementary Table S5). In TP4, the same comparisons were still significant (p-value = 0.047 and p-value = 0.031) although the p-values were smaller. Moreover, the comparison between *Rb1* and *Rb1Rb2* groups also resulted in significance at the last time point (p-value = 0.016; Figure 10).

Interestingly, trees with both RB QTL had the deepest root systems in TP1 with roots reaching an average depth of 332 mm and the group of trees with only *Rb2* had the shallowest root systems with an average depth of 307 mm. However, this completely changed at TP2 where the *Rb1Rb2* group had the shallowest root system with 570 mm mean depth and the *Rb2* group root systems reached a mean depth of 647 mm. The *Rb1Rb2* group stayed as the group with the shallowest root systems during the rest of the experiment. Nevertheless, the deepest root systems in TP3 were found in rootstocks with no RB QTL and in TP4 in trees with only *Rb1* but very similar in depth to NoRb and *Rb2* groups (Supplementary Table S4).

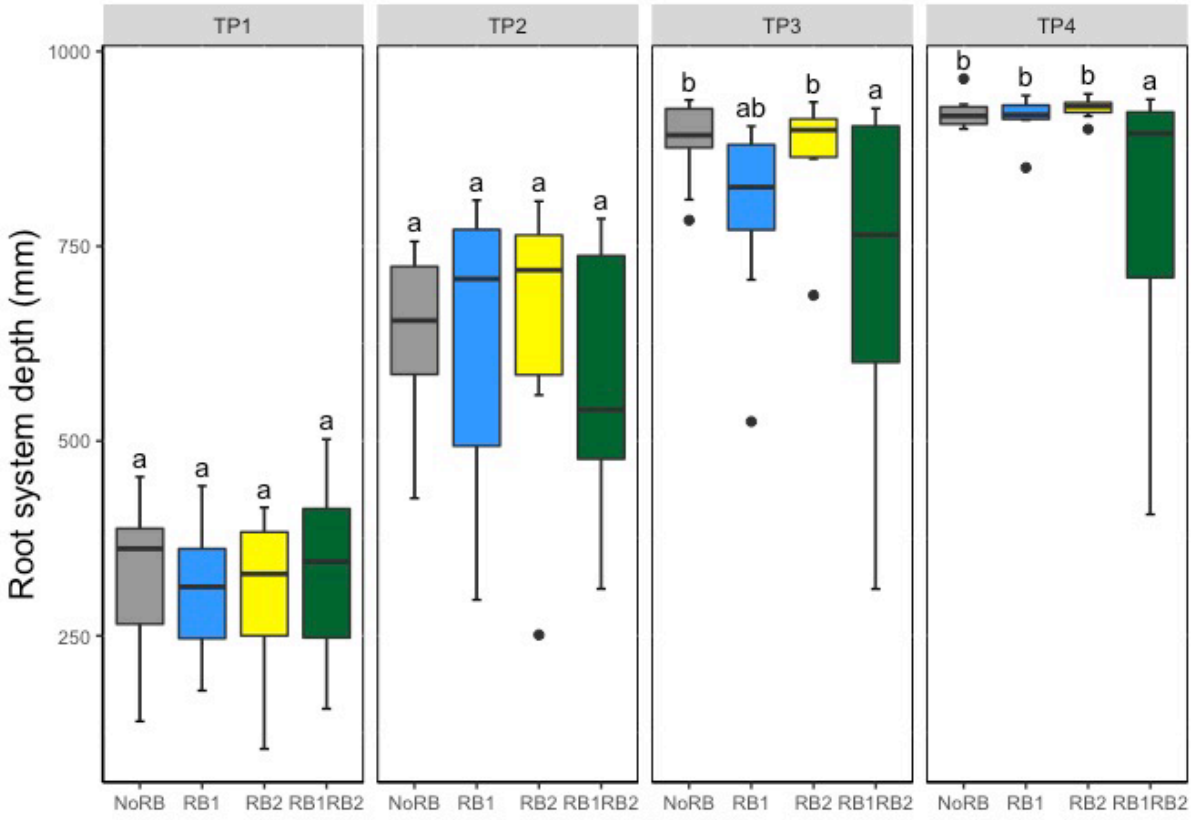

Figure 10. Maximum root system depth of grafted rootstocks with different combinations of root bark QTL per time point. Centerlines show the medians; whiskers mark the maximum and minimum values, respectively. Upper and lower box boundaries represent the 25th and 75th percentiles, respectively. Different lower-case letters are significantly different ($p<0.05$).

4.2.3. Effect of RB QTL on convex hull area (chull area)

The effect of the RB QTL on the convex hull area during the first growing season was analysed using REML analysis. Block, time point and the interactions *Rb1* x TP and *Rb1* x *Rb2* x TP were significant in the model (p-value = 6.67e-05, < 2.2e-16, 0.002 and 0.025, respectively; Table 5). Significant differences in convex hull area between dwarfing categories were observed in TP3, revealing that dwarfing had an impact on the convex hull area in apple rootstocks from the second half of the first growing season. In TP3,

significant differences were found when comparing NoRb and *Rb1Rb2* groups (p-value = 0.0051) and between *Rb2* and *Rb1Rb2* groups (p-value = 0.037). The same comparisons resulted in significant differences in TP4 (p-value = 0.012 and p-value = 0.014, respectively) and, in the comparison between *Rb1* and *Rb1Rb2* groups (p-values = 0.0088; Figure 11; Supplementary Table S7). Similar to root depth, in TP1 the group with both QTL showed the largest root systems whereas in TP2 exhibited the smallest root area, remaining the smallest for the rest of the experiment (Supplementary Table S6).

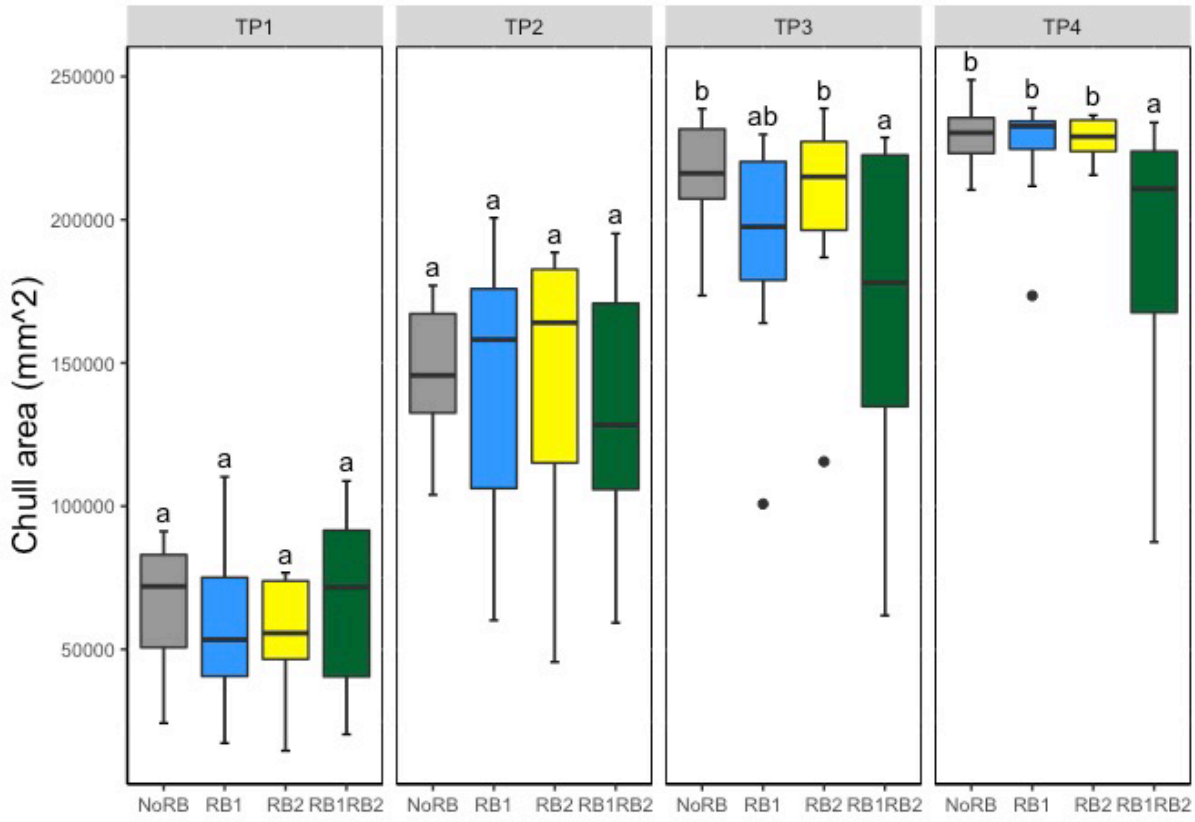

Figure 11. Total convex hull area of grafted rootstocks with different combinations of root bark QTL per time point. Centerlines show the medians; whiskers mark the maximum and minimum values, respectively. Upper and lower box boundaries represent the 25th and 75th percentiles, respectively. Different lower-case letters are significantly different ($p<0.05$).

Table 5. Summary table of the means and ANOVA of total root length, maximum root diameter, mean root diameter, root system depth and total convex hull area per fixed variable including *Rb1, Rb2*, time point, block and their interactions.

		Means		
Fixed variables	**Levels**	**Total root length**	**Root system depth**	**Total convex hull area**
Rb1	**No**	106	688	159649
	Yes	100	638	147580
Rb2	**No**	106	682	159700
	Yes	100	644	147530
TP	**TP1**	51.9	323	61789
	TP2	85.3	622	141328
	TP3	126.3	816	193613
	TP4	149.1	890	217730
Block	**A**	102.4	658	152953
	B	108.9	728	169157
	C	109.7	727	173761
	D	91.6	539	118589
ANOVA				
$\mathbf{F}_{Rb1}$		0.8394 (0.36)	3.44 (*0.07*)	2.34 (0.13)
$\mathbf{F}_{Rb2}$		0.741 (0.39)	1.98 (0.16)	2.39 (0.13)

F_{TP}	261.467 (**<2e-16**)	424.72 (**< 2.2e-16**)	470.28 (**< 2.2e-16**)
F_{B}	1.827 (0.16)	10.89 (**4.32e-05**)	10.309 (**6.67e-05**)
$F_{Rb1xRb2}$	0.329 (0.57)	1.98 (0.16)	1.03 (0.31)
F_{Rb1xTP}	0.986 (0.40)	4.66 (**0.004**)	5.22 (**0.002**)
F_{Rb2xTP}	1.337 (0.26)	1.08 (0.35)	1.76 (0.15)
$F_{Rb1xRb2xTP}$	1.685 (0.17)	2.43 (0.06)	3.23 (**0.025**)

F_{RB1}:Rb1 QTL effect; F_{RB2}:Rb2 QTL effect; F_{TP}:time point effect; F_{B}:block effect; $F_{Rb1xRb2}$:Rb1 x Rb2 QTL interaction effect; F_{Rb1xTP}:Rb1 QTL x time point interaction effect; F_{Rb2xTP}:Rb2 QTL x time point interaction effect; $F_{Rb1xRb2xTP}$:Rb1 x Rb2 x TP interaction effect. P-values in brackets and significant p-values in bold.

5. Discussion

The research presented in this thesis has narrowed the *Rb1* QTL region located in chromosome 5 from 4.4 Mb to 2.2 Mb using the SSR markers specifically developed during this project. The lack of highly polymorphic SSRs has been a challenge for fine-mapping this area.

In addition, two regions linked to rootstock-induced dwarfing have been identified within the *Rb2* region in this study, one located between 6.9 Mb to 7.5 Mb and the second placed between 10.9 Mb to 12.7 Mb. This key finding could offer an explanation for the discrepancies observed in the mapping of *Dw2* on Chromosome 11 by different authors (Fazio *et al.*, 2014; Foster *et al.*, 2015). It also helps to explain the challenges

encountered in the fine mapping of this particular region. Tracking the origin of these two QTL regions using a wider set of germplasm would be key to better understand the genetic source of rootstock-induced dwarfing.

One of the greatest achievements of this PhD is the development of multiplexes of primers for highly polymorphic SSR markers that spanned the QTL regions, providing more complete information than the use of single markers. The estimation of dwarfing haplotypes in the *Rb1* and *Rb2* areas has facilitated the early selection of dwarfing rootstocks for breeders and has shed light on some incongruences derived from the use of unique markers that were finally not closely linked to the dwarfing genes.

Another relevant contribution of this thesis has been the generation of genotypes with recombination points situated in key regions. These genotypes exhibit completely opposite phenotypes (very dwarfing vs vigorous) despite showing recombinations in the same areas. Therefore, the screening of new genetic markers spanning the reduced QTL regions on these key genotypes would help to identify a more specific location of the recombination points and, consequently, would contribute to the further refinement of the root bark QTL.

Rootstock breeding often involves a trade-off between different traits such as vigour, disease resistance and fruit quality. Developing rootstocks that excel in multiple areas while maintaining resilience remains a challenge. Furthermore, there is little research about dwarfing influence on root systems in rootstocks mainly due to difficulties in accessing root systems. While rhizobox experiments may not perfectly mimic field behaviour, they serve as a powerful tool for preliminary investigations and hypothesis generation, providing controlled and reproducible conditions which can be further validated and applied in field conditions. A few studies have revealed that dwarfing rootstocks often showed shallower root systems compared to vigorous rootstocks (Lo Bianco *et al.*, 2003; Ma *et al.*, 2013).

One of the main research questions in this investigation was how dwarfing rootstock influences root system architecture traits that could improve resilience in future climate conditions and whether dwarfing and root architecture can be decoupled. A recent study identified 25 QTL for root angle in apple rootstocks that did not colocalize with the dwarfing QTL, indicating that although dwarfing may influence root angle, it is not genetically controlling it (Zheng *et al.*, 2020). In addition, a study using M.9 and SH.40 apple rootstocks, dwarfing and very dwarfing apple rootstocks respectively, revealed that the SH.40 rootstock exhibited deeper root systems than M.9 despite being more dwarfing. This suggests that there are possibilities for root improvement while keeping a reduced tree size (An *et al.*, 2017a; Ma *et al.*, 2013). In this thesis, dwarfing rootstocks exhibited significantly smaller convex hull area and root system depth compared to vigorous genotypes. Interestingly, the group of rootstocks containing both root bark QTL showed great data variability suggesting that either dwarfing rootstocks are more susceptible to environmental factors or there are other genes controlling root architecture in rootstocks. Consequently, despite the undeniable impact of dwarfing on root architecture, this study suggests that there is an opportunity for enhancing root systems in dwarfing rootstocks.

The root system architecture study has also increased our knowledge about the methodology to evaluate root architecture in trees and how this could be improved to better explore tree root systems. Future experiments should be ideally conducted for a longer period of time to be able to track further differences in root growth between dwarfing and vigorous rootstocks. Furthermore, it would be interesting to include more time points to capture in detail the root development processes and how these correlate to canopy growth over time in dwarfing versus vigorous rootstocks. Lastly, the use of bigger rhizoboxes in future experiments would be essential for analysing the root architecture of trees and prevent vigorous genotypes from running out of space before the end of the experiment.

In addition, the findings of this research could also have a significant potential impact on other high-value perennial crops including cherry, pear and apricot. In pears, a QTL mapping for rootstock-induced dwarfing identified a QTL which is synthetic to *Dw1* in

apples demonstrating the high degree of similarity between apple and pear genomes (Knäbel *et al.*, 2015).

In summary, breeding efforts also focus on enhancing the rootstock resilience to abiotic stresses, such as drought, extreme temperatures, and poor soil conditions. This can involve selecting rootstock varieties that have an improved capacity for water and nutrient uptake, as well as the ability to adapt to adverse soil conditions using genetic markers tightly linked to the relevant traits. Developing rootstocks with efficient root systems that can explore a larger soil volume for resources and maintain stable water uptake under varying environmental conditions is a key objective.

6. References

An, H., Dong, H., Wu, T., Wang, Y., Xu, X., Zhang, X. and Han, Z. (2017a). Root growth angle: An important trait that influences the deep rooting of apple rootstocks. *Scientia horticulturae*, 216, p.256–263. [Online]. Available at: doi:10.1016/j.scienta.2017.01.019.

An, H., Luo, F., Wu, T., Wang, Y., Xu, X., Zhang, X. and Han, Z. (2017b). Dwarfing Effect of Apple Rootstocks Is Intimately Associated with Low Number of Fine Roots. *HortScience : a publication of the American Society for Horticultural Science*, 52 (4), p.503–512. [Online]. Available at: doi:10.21273/HORTSCI11579-16.

Atkinson, C. J. and Else, M. (2001). Understanding how rootstocks dwarf fruit trees. *Compact Fruit Tree*, (34), p.46–49.

Bates, D., Mächler, M., Bolker, B. and Walker, S. (2015). Fitting linear mixed-effects models using lme4. *Journal of Statistical Software*, 67 (1), p.1–48. [Online]. Available at: doi:10.18637/jss.v067.i01.

Beakbane, A. B. and Thompson, E. C. (1947). Anatomical studies of stems and roots of hardy fruit trees. IV. the root structure of some new clonal apple rootstocks budded with cox's orange pippin. *Journal of Pomology and Horticultural Science*, 23 (4), p.206–211. [Online]. Available at: doi:10.1080/03683621.1947.11513669.

Bohn, M., Novais, J., Fonseca, R., Tuberosa, R. and Grift, T. E. (2006). Genetic evaluation of root complexity in maize. *Acta Agronomica Hungarica*, 54 (3), p.291–303. [Online]. Available at: doi:10.1556/AAgr.54.2006.3.3.

Boutin-Ganache, I., Raposo, M., Raymond, M. and Deschepper, C. F. (2001). M13-tailed primers improve the readability and usability of microsatellite analyses performed with two different allele-sizing methods. *Biotechniques*, 31 (1), p.24–26, 28. [Online]. Available at: doi:10.2144/01311bm02.

Costes, E. and Lauri, P. E. (1995). Processus de croissance en relation avec la ramification sylleptique et la floraison chez le pommier. *J. Bouchon (ed.), Architecture des arbresfruitiers et forestiers. INRA Editions*, 74, p.41–50.

De Silva, H. (1999). Analysis of distribution of root length density of apple trees on different dwarfing rootstocks. *Annals of Botany*, 83 (4), p.335–345. [Online]. Available at: doi:10.1006/anbo.1999.0829.

Edge-Garza, D. A., Rowland, T. V., Haendiges, S. and Peace, C. (2014). A high-throughput and cost-efficient DNA extraction protocol for the tree fruit crops of apple,

sweet cherry, and peach relying on silica beads during tissue sampling. *Molecular Breeding*, 34 (4), p.2225–2228. [Online]. Available at: doi:10.1007/s11032-014-0160-x.

Fazio, G., Wan, Y., Kviklys, D., Romero, L., Adams, R., Strickland, D. and Robinson, T. (2014). Dw2, a new dwarfing locus in apple rootstocks and its relationship to induction of early bearing in apple scions. *Journal of the American Society for Horticultural Science*, 139 (2), p.87–98. [Online]. Available at: doi:10.21273/JASHS.139.2.87.

Foster, T. M., Celton, J.-M., Chagné, D., Tustin, D. S. and Gardiner, S. E. (2015). Two quantitative trait loci, Dw1 and Dw2, are primarily responsible for rootstock-induced dwarfing in apple. *Horticulture Research*, 2, p.15001. [Online]. Available at: doi:10.1038/hortres.2015.1.

García-Villanueva, E., Costes, E. and Jourdan, C. (2004). Comparing root and aerial growth dynamics of two apple hybrids ownrooted and grafted on m.9. *Acta horticulturae*, (658), p.61–67. [Online]. Available at: doi:10.17660/ActaHortic.2004.658.5.

Graves, S., Piepho, H. P., Selzer, L. and Dorai-Raj, S. (2019). multcompView: Visualizations of Paired Comparisons. *R package version 0.1-8*. [Online]. Available at: https://cran.r-project.org/web/packages/multcompView/index.html [Accessed: 1 June 2022].

Harrison, N., Harrison, R. J., Barber-Perez, N., Cascant-Lopez, E., Cobo-Medina, M., Lipska, M., Conde-Ruíz, R., Brain, P., Gregory, P. J. and Fernández-Fernández, F. (2016). A new three-locus model for rootstock-induced dwarfing in apple revealed by genetic mapping of root bark percentage. *Journal of Experimental Botany*, 67 (6), p.1871–1881. [Online]. Available at: doi:10.1093/jxb/erw001.

Hodge, A. (2004). The plastic plant: root responses to heterogeneous supplies of nutrients. *The New Phytologist*, 162 (1), p.9–24. [Online]. Available at: doi:10.1111/j.1469-8137.2004.01015.x.

Hothorn, T., Bretz, F. and Westfall, P. (2008). Simultaneous inference in general parametric models. *Biometrical Journal. Biometrische Zeitschrift*, 50 (3), p.346–363. [Online]. Available at: doi:10.1002/bimj.200810425.

Hou, C., Ma, L., Luo, F., Wang, Y., Zhang, X. and Han, Z. (2012). Impact of rootstock and interstems on fine root survivorship and seasonal variation in apple. *Scientia horticulturae*, 148, p.169–176. [Online]. Available at: doi:10.1016/j.scienta.2012.10.008.

Jensen, P. J., Halbrendt, N., Fazio, G., Makalowska, I., Altman, N., Praul, C., Maximova, S. N., Ngugi, H. K., Crassweller, R. M., Travis, J. W. and McNellis, T. W. (2012). Rootstock-regulated gene expression patterns associated with fire blight resistance in apple. *BMC Genomics*, 13, p.9. [Online]. Available at: doi:10.1186/1471-2164-13-9.

Karlova, R., Boer, D., Hayes, S. and Testerink, C. (2021). Root plasticity under abiotic stress. *Plant Physiology*, 187 (3), p.1057–1070. [Online]. Available at: doi:10.1093/plphys/kiab392.

Knäbel, M., Friend, A. P., Palmer, J. W., Diack, R., Wiedow, C., Alspach, P., Deng, C., Gardiner, S. E., Tustin, D. S., Schaffer, R., Foster, T. and Chagné, D. (2015). Genetic control of pear rootstock-induced dwarfing and precocity is linked to a chromosomal region syntenic to the apple Dw1 loci. *BMC Plant Biology*, 15, p.230. [Online]. Available at: doi:10.1186/s12870-015-0620-4.

Koevoets, I. T., Venema, J. H., Elzenga, J. T. M. and Testerink, C. (2016). Roots Withstanding their Environment: Exploiting Root System Architecture Responses to Abiotic Stress to Improve Crop Tolerance. *Frontiers in Plant Science*, 7, p.1335. [Online]. Available at: doi:10.3389/fpls.2016.01335.

Lenth, R., Singmann, H., Love, J., Buerkner, P. and Herve, M. (2018). Package "Emmeans." *R package version 4.0-3*.

Liebhard, R., Gianfranceschi, L., Koller, B., Ryder, C. D., Tarchini, R., Van De Weg, E. and Gessler, C. (2002). Development and characterisation of 140 new microsatellites in apple (Malus x domestica Borkh.). *Molecular Breeding*.

Li, H., Handsaker, B., Wysoker, A., Fennell, T., Ruan, J., Homer, N., Marth, G., Abecasis, G., Durbin, R. and 1000 Genome Project Data Processing Subgroup. (2009). The Sequence Alignment/Map format and SAMtools. *Bioinformatics*, 25 (16), p.2078–2079. [Online]. Available at: doi:10.1093/bioinformatics/btp352.

Lo Bianco, R., Policarpo, M. and Scariano, L. (2003). Effects of rootstock vigour and in-row spacing on stem and root growth, conformation and dry-matter distribution of young apple trees. *The Journal of Horticultural Science and Biotechnology*, 78 (6), p.828–836. [Online]. Available at: doi:10.1080/14620316.2003.11511705.

López-Bucio, J., Cruz-Ramírez, A. and Herrera-Estrella, L. (2003). The role of nutrient availability in regulating root architecture. *Current Opinion in Plant Biology*, 6 (3), p.280–287. [Online]. Available at: doi:10.1016/S1369-5266(03)00035-9.

Ludlow, M. M. and Muchow, R. C. (1990). A Critical Evaluation of Traits for Improving Crop Yields in Water-Limited Environments. In: *Advances in agronomy volume 43*, Advances in Agronomy, 43, Elsevier, p.107–153. [Online]. Available at: doi:10.1016/S0065-2113(08)60477-0.

Lynch, J. P. (1995). Root architecture and plant productivity. *Plant Physiology*, 109 (1), p.7–13. [Online]. Available at: doi:10.1104/pp.109.1.7.

Lynch, J. P. (2007). Roots of the Second Green Revolution. *Australian journal of botany*, 55 (5), p.493. [Online]. Available at: doi:10.1071/BT06118.

Maggs, D. H. (1955). The inception of flowering in some apple rootstock varieties. *Journal of Horticultural Science*, 30 (4), p.234–241. [Online]. Available at: doi:10.1080/00221589.1955.11513846.

Malamy, J. E. (2005). Intrinsic and environmental response pathways that regulate root system architecture. *Plant, Cell & Environment*, 28 (1), p.67–77. [Online]. Available at: doi:10.1111/j.1365-3040.2005.01306.x.

Marguerit, E., Brendel, O., Lebon, E., Van Leeuwen, C. and Ollat, N. (2012). Rootstock control of scion transpiration and its acclimation to water deficit are controlled by different genes. *The New Phytologist*, 194 (2), p.416–429. [Online]. Available at: doi:10.1111/j.1469-8137.2012.04059.x.

Ma, L., Hou, C. W., Zhang, X. Z., Li, H. L., Han, D. G., Wang, Y. and Han, Z. H. (2013). Seasonal growth and spatial distribution of apple tree roots on different rootstocks or interstems. *Journal of the American Society for Horticultural Science*, 138 (2), p.79–87. [Online]. Available at: doi:10.21273/JASHS.138.2.79.

Osmont, K. S., Sibout, R. and Hardtke, C. S. (2007). Hidden branches: developments in root system architecture. *Annual review of plant biology*, 58, p.93–113. [Online]. Available at: doi:10.1146/annurev.arplant.58.032806.104006.

Paez-Garcia, A., Motes, C. M., Scheible, W.-R., Chen, R., Blancaflor, E. B. and Monteros, M. J. (2015). Root traits and phenotyping strategies for plant improvement. *Plants*, 4 (2), p.334–355. [Online]. Available at: doi:10.3390/plants4020334.

Pilcher, R. L. R., Celton, J. M., Gardiner, S. E. and Tustin, D. S. (2008). Genetic Markers Linked to the Dwarfing Trait of Apple Rootstock 'Malling 9.' *Journal of the American Society for Horticultural Science*.

Robinson, T. L. (2007). Effects of tree density and tree shape on apple orchard performance. *Acta horticulturae*, (732), p.405–414. [Online]. Available at: doi:10.17660/ActaHortic.2007.732.61.

van Rossum, G. (1995). Python reference manual. *Centrum voor Wiskunde en Informatica Amsterdam.*

Schindelin, J., Arganda-Carreras, I., Frise, E., Kaynig, V., Longair, M., Pietzsch, T., Preibisch, S., Rueden, C., Saalfeld, S., Schmid, B., Tinevez, J.-Y., White, D. J., Hartenstein, V., Eliceiri, K., Tomancak, P. and Cardona, A. (2012). Fiji: an open-source platform for biological-image analysis. *Nature Methods*, 9 (7), p.676–682. [Online]. Available at: doi:10.1038/nmeth.2019.

Seleznyova, A. N., Thorp, T. G., White, M., Tustin, S. and Costes, E. (2003). Application of architectural analysis and AMAPmod methodology to study dwarfing phenomenon: the branch structure of “Royal Gala” apple grafted on dwarfing and non-dwarfing rootstock/interstock combinations. *Annals of Botany*, 91 (6), p.665–672. [Online]. Available at: doi:10.1093/aob/mcg072.

Tamura, F. (2012). Recent advances in research on japanese pear rootstocks. *Journal of the Japanese Society for Horticultural Science*, 81 (1), p.1–10. [Online]. Available at: doi:10.2503/jjshs1.81.1.

Tworkoski, T. and Fazio, G. (2015). Effects of Size-Controlling Apple Rootstocks on Growth, Abscisic Acid, and Hydraulic Conductivity of Scion of Different Vigor. *International Journal of Fruit Science*, 15 (4), p.369–381. [Online]. Available at: doi:10.1080/15538362.2015.1009973.

Untergasser, A., Cutcutache, I., Koressaar, T., Ye, J., Faircloth, B. C., Remm, M. and Rozen, S. G. (2012). Primer3--new capabilities and interfaces. *Nucleic Acids Research*, 40 (15), p.e115. [Online]. Available at: doi:10.1093/nar/gks596.

Webster, A. D. (1995a). Rootstock and interstock effects on deciduous fruit tree vigour, precocity, and yield productivity. *New Zealand journal of crop and horticultural science*, 23 (4), p.373–382. [Online]. Available at: doi:10.1080/01140671.1995.9513913.

Webster, A. D. (1995b). Temperate fruit tree rootstock propagation. *New Zealand journal of crop and horticultural science*, 23 (4), p.355–372. [Online]. Available at: doi:10.1080/01140671.1995.9513912.

van der Weele, C. M., Spollen, W. G., Sharp, R. E. and Baskin, T. I. (2000). Growth of Arabidopsis thaliana seedlings under water deficit studied by control of water potential in nutrient-agar media. *Journal of Experimental Botany*, 51 (350), p.1555–1562. [Online]. Available at: doi:10.1093/jexbot/51.350.1555.

Wickham, H. (2016). *ggplot2 - Elegant Graphics for Data Analysis*. 2nd ed. Cham: Springer International Publishing. [Online]. Available at: doi:10.1007/978-3-319-24277-4.

Zheng, C., Shen, F., Wang, Y., Wu, T., Xu, X., Zhang, X. and Han, Z. (2020). Intricate genetic variation networks control the adventitious root growth angle in apple. *BMC Genomics*, 21 (1), p.852. [Online]. Available at: doi:10.1186/s12864-020-07257-8.

Supplementary Data

Supplementary Table S1. Plot name, location, planting year, parentage and number of trees sampled per scion from breeding trials used for fine mapping the root bark QTL.

Plot name	Planting year	Genotype	Pedigree	N. trees sampled Scion A*	N. trees sampled Scion B**
RF185	2012	M.9	Unknown	3	-
RF185	2012	M.M.106	Northern Spy x M.1	4	-
RF185	2012	M.116	M.27 x M.M.106	4	-
RF185	2012	M306-6	AR86-1-20 x M.20	3	-
RF185	2012	M306-79	AR86-1-20 x M.20	4	-
RF185	2012	M306-189	AR86-1-20 x M.20	4	-
VF224	2010	AR10-3-9	M.M106 x M.27	7	-
VF224	2010	AR809-3	R80 x M.26	8	-
VF224	2010	AR835-11	M793 x M.9	7	-
VF224	2010	M.116	M.27 x M.M.106	8	-
VF224	2010	M.M.106	Northern Spy x M.1	8	-
VF224	2010	R80	AR134-31 x AR86-1-22	8	-
EE207	2010	AR852-3	AR362-16 x OP***	5	3
EE207	2010	AR839-9	M.7 x M.27	8	6
EE207	2010	B24	AR10-2-5 x AR86-1-22	5	5
EE207	2010	M.26	M.16 x M.9	8	7
EE207	2010	M.27	M.13 x M.9	8	4

EE207	2010	M.9	Unknown	7	6
EE207	2010	R104	AR134-31 x AR86-1-22	4	3
EE207	2010	R59	AR134-31 x AR86-1-22	7	6
SP250	2014	SJM15	*M. baccata 'Nertchinsk'* x M.9	0	3
SP250	2014	SJM167	*M. baccata 'Nertchinsk'* x M.26	4	4
SP250	2014	SJM188	*M. baccata 'Nertchinsk'* x M.26	3	0
SP250	2014	SJM189	*M. baccata 'Nertchinsk'* x M.26	0	4
SP250	2014	SJP84-5162	*M. robusta 5* x M.27	3	0
SP250	2014	SJP84-5174	*M. robusta 5* x M.27	2	2
SP250	2014	SJP84-5217	*M. robusta 5* x B.57490	4	4
SP250	2014	SJP84-5231	*M. robusta 5* x M.27	0	2
SP250	2014	M.26	M.16 x M.9	4	4
SP250	2014	M.9	Unknown	3	4
SP250	2014	M.M.106	Northern Spy x M.1	4	4

* RF185 rootstocks and VF224 rootstocks were only grafted using one scion, Gala and Red Falstaff, respectively. For EE207 and SP250 plots, scion A was Braeburn.

**Scion B was Royal Gala for rootstocks in EE207 plot and Gala for rootstocks in SP250 plot.

***Open pollination (pollen donor unknown)

Supplementary Table S2. Estimated marginal means (EMMs) for linear mixed model of each root bark QTL group within each time point for total root length in the root architecture experiment. Results are averaged over the levels of: block. Degrees of freedom method: Kenward-roger. Confidence level used: 0.95

TP	RB QTL group	emmean	SE	df	Lower.CL	Upper.CL
TP1	**NoRb**	56.3	8.00	70.3	40.3	72.3
TP1	***Rb1***	48.2	7.59	70.2	33.0	63.3
TP1	***Rb2***	50.0	8.46	70.6	33.1	66.9
TP1	***Rb1Rb2***	52.9	6.91	70.6	39.2	66.7
TP2	**NoRb**	86.0	8.00	70.3	70.0	101.9
TP2	***Rb1***	87.9	7.59	70.2	72.8	103.1
TP2	***Rb2***	84.9	8.46	70.6	68.1	101.8
TP2	***Rb1Rb2***	82.5	6.91	70.6	68.7	96.3
TP3	**NoRb**	126.7	8.00	70.3	110.8	142.7
TP3	***Rb1***	128.8	7.59	70.2	113.7	144.0
TP3	***Rb2***	134.0	8.46	70.6	117.1	150.9
TP3	***Rb1Rb2***	115.6	6.91	70.6	101.8	129.4
TP4	**NoRb**	158.6	8.00	70.3	142.6	174.5
TP4	***Rb1***	154.1	7.59	70.2	138.9	169.2
TP4	***Rb2***	151.5	8.46	70.6	134.7	168.4
TP4	***Rb1Rb2***	132.2	6.91	70.6	118.4	146.0

Supplementary Table S3. Multiple comparison test of root bark QTL groups within each time point for total root length in the root architecture experiment. Results are averaged over the levels of: Block. Degrees-of-freedom method: kenward-roger. P value adjustment: tukey method for comparing a family of 4 estimates. Significant p-values in bold.

TP	contrast	estimate	SE	df	t.ratio	p.value
TP1	**NoRb – *Rb1***	8.10	11.0	70.1	0.734	0.8833
TP1	**NoRb – *Rb1Rb2***	3.35	10.6	70.4	0.317	0.9889
TP1	**NoRb – *Rb2***	6.31	11.6	70.5	0.542	0.9483
TP1	***Rb1* – *Rb1Rb2***	-4.76	10.3	70.4	-0.463	0.9668
TP1	***Rb1* – *Rb2***	-1.79	11.4	70.4	-0.157	0.9986
TP1	***Rb1Rb2* – *Rb2***	-2.97	10.9	70.6	-0.271	0.9929
TP2	**NoRb – *Rb1***	-1.96	11.0	70.1	-0.177	0.9980
TP2	**NoRb – *Rb1Rb2***	3.46	10.6	70.4	0.327	0.9878
TP2	**NoRb – *Rb2***	1.04	11.6	70.5	0.089	0.9997
TP2	***Rb1* – *Rb1Rb2***	5.42	10.3	70.4	0.528	0.9520
TP2	***Rb1* – *Rb2***	3.00	11.4	70.4	0.264	0.9935
TP2	***Rb1Rb2* – *Rb2***	2.42	10.9	70.6	0.222	0.9961
TP3	**NoRb – *Rb1***	-2.09	11.0	70.1	-0.189	0.9976
TP3	**NoRb – *Rb1Rb2***	11.11	10.6	70.4	1.051	0.7204
TP3	**NoRb – *Rb2***	-7.30	11.6	70.5	-0.627	0.9230
TP3	***Rb1* – *Rb1Rb2***	13.20	10.3	70.4	1.285	0.5751
TP3	***Rb1* – *Rb2***	-5.21	11.4	70.4	-0.458	0.9678

TP3	***Rb1Rb2 – Rb2***	18.41	10.9	70.6	1.685	0.3392
TP4	**NoRb – *Rb1***	4.49	11.0	70.1	0.407	0.9771
TP4	**NoRb – *Rb1Rb2***	26.39	10.6	70.4	2.497	*0.0691*
TP4	**NoRb – *Rb2***	7.05	11.6	70.5	0.606	0.9299
TP4	***Rb1 – Rb1Rb2***	21.90	10.3	70.4	2.133	0.1527
TP4	***Rb1 – Rb2***	2.56	11.4	70.4	0.225	0.9959
TP4	***Rb1Rb2 – Rb2***	19.34	10.9	70.6	1.770	0.2961

Supplementary Table S4. Estimated marginal means (EMMs) for linear mixed model of each root bark QTL group within each time point for maximum root depth in the root architecture experiment. Results are averaged over the levels of: block. Degrees of freedom method: Kenward-roger. Confidence level used: 0.95.

TP	RB QTL group	emmean	SE	df	Lower.CL	Upper.CL
TP1	**NoRb**	329	35.6	74.3	258	400
TP1	***Rb1***	324	33.8	74.2	257	392
TP1	***Rb2***	307	37.7	74.6	232	382
TP1	***Rb1Rb2***	332	30.8	74.6	271	393
TP2	**NoRb**	632	35.6	74.3	561	703
TP2	***Rb1***	640	33.8	74.2	573	708
TP2	***Rb2***	647	37.7	74.6	572	723
TP2	***Rb1Rb2***	570	30.8	74.6	508	631
TP3	**NoRb**	877	35.6	74.3	806	948
TP3	***Rb1***	810	33.8	74.2	743	877
TP3	***Rb2***	872	37.7	74.6	797	947
TP3	***Rb1Rb2***	705	30.8	74.6	644	767
TP4	**NoRb**	915	35.6	74.3	844	986
TP4	***Rb1***	929	33.8	74.2	862	997
TP4	***Rb2***	927	37.7	74.6	852	1002
TP4	***Rb1Rb2***	790	30.8	74.6	728	851

Supplementary Table S5. Multiple comparison test of root bark QTL groups within each time point for maximum root depth in the root architecture experiment. Results are averaged over the levels of: Block. Degrees-of-freedom method: kenward-roger. P value adjustment: tukey method for comparing a family of 4 estimates. Significant p-values in bold.

TP	contrast	estimate	SE	df	t.ratio	p.value
TP1	**NoRb – *Rb1***	4.68	49.2	74.0	0.095	0.9997
TP1	**NoRb – *Rb1Rb2***	-2.84	47.1	74.4	-0.060	0.9999
TP1	**NoRb – *Rb2***	22.41	51.9	74.5	0.0432	0.9728
TP1	***Rb1* – *Rb1Rb2***	-7.52	45.7	74.4	-0.164	0.9984
TP1	***Rb1* – *Rb2***	17.72	50.7	74.4	0.350	0.9852
TP1	***Rb1Rb2* – *Rb2***	-25.24	48.7	74.6	-0.519	0.9544
TP2	**NoRb – *Rb1***	-7.99	49.2	74.0	-0.162	0.9985
TP2	**NoRb – *Rb1Rb2***	62.64	47.1	74.4	1.330	0.5470
TP2	**NoRb – *Rb2***	-15.08	51.9	74.5	-0.291	0.9914
TP2	***Rb1* – *Rb1Rb2***	70.63	45.7	74.4	1.544	0.4168
TP2	***Rb1* – *Rb2***	-7.09	50.7	74.4	-0.140	0.9990
TP2	***Rb1Rb2* – *Rb2***	77.72	48.7	74.6	1.597	0.3867
TP3	**NoRb – *Rb1***	66.54	49.2	74.0	1.352	0.5333
TP3	**NoRb – *Rb1Rb2***	171.20	47.1	74.4	3.635	**0.0028**
TP3	**NoRb – *Rb2***	4.24	51.9	74.5	0.082	0.9998
TP3	***Rb1* – *Rb1Rb2***	104.66	45.7	74.4	2.288	0.1101
TP3	***Rb1* – *Rb2***	-62.30	50.7	74.4	-1.230	0.6100

TP3	***Rb1Rb2 – Rb2***	166.96	48.7	74.6	3.430	**0.0053**
TP4	**NoRb – *Rb1***	-14.53	49.2	74.0	-0.295	0.9910
TP4	**NoRb – *Rb1Rb2***	124.92	47.1	74.4	2.653	**0.0471**
TP4	**NoRb – *Rb2***	-12.05	51.9	74.5	-0.232	0.9956
TP4	***Rb1 – Rb1Rb2***	139.45	45.7	74.4	3.049	**0.0164**
TP4	***Rb1 – Rb2***	2.49	50.7	74.4	0.049	1.0000
TP4	***Rb1Rb2 – Rb2***	136.97	48.7	74.6	2.814	**0.0311**

Supplementary Table S6. Estimated marginal means (EMMs) for linear mixed model of each root bark QTL group within each time point for convex hull area in the root architecture experiment. Results are averaged over the levels of: block. Degrees of freedom method: Kenward-roger. Confidence level used: 0.95

TP	RB QTL group	emmean	SE	df	Lower.CL	Upper.CL
TP1	**NoRb**	64101	9905	66.1	44327	83876
TP1	***Rb1***	62415	9402	66.0	43643	81187
TP1	***Rb2***	54555	10476	66.4	33642	75468
TP1	***Rb1Rb2***	66086	8553	66.4	49010	83161
TP2	**NoRb**	143943	9905	66.1	124169	163718
TP2	***Rb1***	145845	9402	66.0	127073	164617
TP2	***Rb2***	144085	10476	66.4	123172	164998
TP2	***Rb1Rb2***	131439	8553	66.4	114364	148514
TP3	**NoRb**	211174	9905	66.1	191399	230948
TP3	***Rb1***	194198	9402	66.0	175426	212970
TP3	***Rb2***	203173	10476	66.4	182260	224086
TP3	***Rb1Rb2***	165906	8553	66.4	148830	182981
TP4	**NoRb**	227695	9905	66.1	207920	247469
TP4	***Rb1***	228228	9402	66.0	209456	247000
TP4	***Rb2***	228470	10476	66.4	207558	249383
TP4	***Rb1Rb2***	186527	8553	66.4	169451	203602

Supplementary Table S7. Multiple comparison test of root bark QTL groups within each time point for convex hull area in the root architecture experiment. Results are averaged over the levels of: Block. Degrees-of-freedom method: kenward-roger. P value adjustment: tukey method for comparing a family of 4 estimates. Significant p-values in bold.

TP	contrast	estimate	SE	df	t.ratio	p.value
TP1	**NoRb – *Rb1***	1686	13680	65.9	0.123	0.9993
TP1	**NoRb – *Rb1Rb2***	-1984	13087	66.2	-0.152	0.9987
TP1	**NoRb – *Rb2***	9546	14417	66.3	0.662	0.9109
TP1	***Rb1* – *Rb1Rb2***	-3671	12711	66.2	-0.289	0.9915
TP1	***Rb1* – *Rb2***	7860	14076	66.2	0.558	0.9439
TP1	***Rb1Rb2* – *Rb2***	-11531	13524	66.4	-0.853	0.8290
TP2	**NoRb – *Rb1***	-1901	13680	65.9	-0.139	0.9990
TP2	**NoRb – *Rb1Rb2***	12504	13087	66.2	0.956	0.7750
TP2	**NoRb – *Rb2***	-141	14417	66.3	-0.010	1.0000
TP2	***Rb1* – *Rb1Rb2***	14406	12711	66.2	1.133	0.6704
TP2	***Rb1* – *Rb2***	1760	14076	66.2	0.125	0.9993
TP2	***Rb1Rb2* – *Rb2***	12646	13524	66.4	0.935	0.7861
TP3	**NoRb – *Rb1***	16975	13680	65.9	1.241	0.6034
TP3	**NoRb – *Rb1Rb2***	45268	13087	66.2	3.459	**0.0051**
TP3	**NoRb – *Rb2***	8001	14417	66.3	0.555	0.9449
TP3	***Rb1* – *Rb1Rb2***	28293	12711	66.2	2.226	0.1269
TP3	***Rb1* – *Rb2***	-8975	14076	66.2	-0.638	0.9195
TP3	***Rb1Rb2* – *Rb2***	37267	13524	66.4	2.756	**0.0370**
TP4	**NoRb – *Rb1***	-534	13680	65.9	-0.039	1.0000
TP4	**NoRb – *Rb1Rb2***	41168	13087	66.2	3.146	**0.0129**

TP4	**NoRb – *Rb2***	-776	14417	66.3	-0.054	0.9999
TP4	***Rb1 – Rb1Rb2***	41702	12711	66.2	3.281	**0.0088**
TP4	***Rb1 – Rb2***	-242	14076	66.2	-0.017	1.0000
TP4	***Rb1Rb2 – Rb2***	41944	13524	66.4	3.101	**0.0147**